

Resonance phenomena in Macroscopic Quantum Tunneling: the small viscosity limit

Yu N Ovchinnikov

L.D. Landau Institute for Theoretical Physics, Academy of Science, Moscow, Russia

S Rombetto [‡]

Università degli Studi di Napoli “Federico II”, Naples, Italy

B Ruggiero

Istituto di Cibernetica “E. Caianiello” del CNR, Pozzuoli (Naples), Italy

V Corato

Dipartimento di Ingegneria dell’Informazione, Seconda Università di Napoli, Naples, Italy

P Silvestrini

E-mail: `paolo.silvestrini@unina2.it`

Dipartimento di Ingegneria dell’Informazione, Seconda Università di Napoli, Naples, Italy

Abstract. We present a new theoretical approach to describe the quantum behavior of a macroscopic system interacting with an external irradiation field, close to the resonant condition. Here we consider the extremely underdamped regime for a system described by a double well potential. The theory includes both: transitions from one well to the other and relaxation processes. We simulate resonant phenomena in a rf-SQUID, whose parameters lie in the range typically used in the experiments. The dependence of the transition probability W on the external drive of the system φ_x shows three resonance peaks. One peak is connected with the resonant tunneling and the two others with the resonant pumping. The relative position of the two peaks correlated to the resonant pumping depends on the pumping frequency ν and on the system parameters. The preliminary measurements on our devices show a low dissipation level and assure that they are good candidates in order to realize new experiments on the resonant phenomena in the presence of an external microwave irradiation of proper frequency.

PACS numbers: 74.50.+r, 03.65.Yz, 03.67.Lx

[‡] also at: Istituto di Cibernetica “E. Caianiello” del CNR, Pozzuoli (Naples), Italy

1. Introduction

Josephson devices are convenient instruments for investigating macroscopic quantum effects [1]. First experiments focused on incoherent phenomena such as macroscopic quantum tunneling (MQT) [2, 3, 4, 5] and energy level quantization (ELQ) [6, 7, 8]. Recent experiments have shown a coherent superposition of distinct macroscopic quantum states in SQUID systems [9, 10, 11] under the action of an external microwave irradiation. These results have stimulated many researchers to search for new quantum phenomena at macroscopic level as well as a method to distinguish them from classical predictions. Moreover quantum effects in SQUID dynamics are interesting because of possible applications to quantum computing [12], as demonstrated by recent experiments [10], [11]. Anyway these results need a final confirmation, since some of them have been reproduced by using a classical model to describe the phenomena [13].

The main problem to observe quantum phenomena at macroscopic level is the interaction with the environment which produces dissipation of coherent effects into classical statistical mixture of quantum states. Among a great variety of incoherent effects, the environment induces a finite width γ of quantum levels [14] and, in this situation, resonant phenomena can occur only if γ is small compared to the energy difference between levels, $\hbar\gamma \ll \hbar\Omega_p$, where

$$\Omega_p = \sqrt{\frac{1}{M} \left(\frac{\partial^2 U}{\partial \varphi^2} \right)_{\varphi=\varphi_{min}}} \quad (1)$$

is the plasma frequency, and φ_{min} is the coordinate corresponding to the minimum of the considered potential well. We have already discussed [15] the behavior of microwave induced transitions in a rf-SQUID in the moderate underdamped regime, when γ is larger than the probability of quantum tunneling under the potential barrier, T_N , ($\gamma \gg T_N$) [16].

In the present paper we extend the theoretical analysis to the small viscosity limit, corresponding to $\gamma \approx T_N$, referred as the *extremely underdamped regime*. In this conditions we can neglect the interwell transitions with respect to the tunneling transitions. Up to now, this regime has been investigated only for other Josephson devices [10, 8]. Here we present a new theory specific for the rf-SQUID, characterized by a double well potential (Fig.1), in order to identify coherent phenomena and to suggest a way of measuring them.

It's worth nothing that Averin et al. [17], [18], [19] already reported a theoretical investigation of resonant quantum phenomena in rf SQUIDs. Nevertheless in that paper all quantities are postulated and not found from the initial Hamiltonian, while we don't not use any fitting parameters, but only external parameter values entering in the Hamiltonian.

We study the interaction between a macroscopic quantum system (the rf-SQUID) and an external microwave irradiation, for frequencies close to resonant conditions.

The probability of a transition under the potential barrier decreases exponentially with

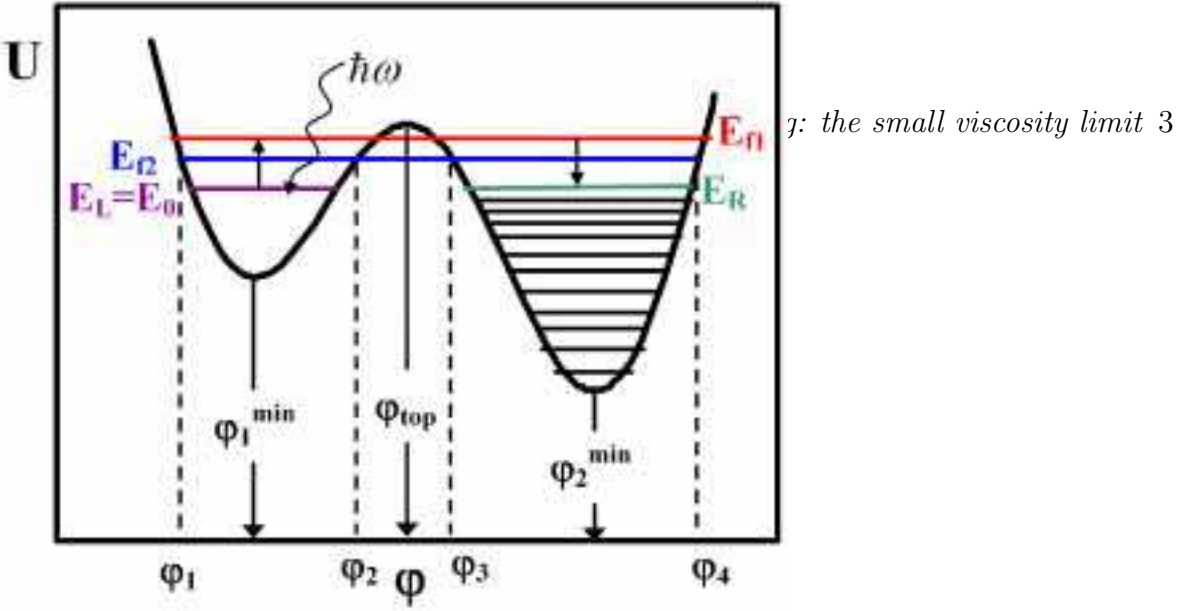


Figure 1. A sketch of an rf-SQUID double-well potential $U(\varphi)$, with two minima located at φ_1^{\min} and φ_2^{\min} . φ_{top} is the position of the potential maximum. The coordinates $\varphi_1, \varphi_2, \varphi_3, \varphi_4$ are the “turning points” of energy E_{f_1} . In the same way it’s possible to define turning points for energies E_{f_2}, E_0, E_R, E_L . We study the case $E_L = E_0$, that is the ground state in the left potential well.

the decreasing energy of the quantum state. Tunneling occurs from a level close to the barrier top. In this case, as we’ll show in the following, the transition probability curve can present three peaks.

A further requirement to observe the quantum tunneling phenomenon is that the number of levels n is not too large, so that no crowding of levels happens. At the same time we assume the number of levels in the potential well is large enough, so that the motion of a particle with energy close to the top of the potential barrier can be considered quasiclassical. In this limit we use approximations reported in [20].

In the quasiclassical limit, the density of levels close to the barrier top increases, but in the considered case this effect is not significant, since numerical factors are of the order of $\frac{1}{2\pi} \ln n$ [20]. Furthermore, near to the barrier top, repulsion of levels is relevant and hence the equation for the system wave functions should be solved exactly. Finally the tunneling probability of a particle through the potential barrier depends very strongly on the particle energy E and on the energy difference between neighboring levels. The position and the width of each level depends on the external parameters of the system. A sketch of the double well potential of the rf-SQUID here studied is reported in Fig.1.

Each macroscopic flux state of the rf-SQUID corresponds to the system wave function confined in one of the two potential wells. By varying the external parameter φ_x it’s possible to control the energy difference between the levels in different wells.

Out of resonance conditions, the energy levels are localized in each well. When two levels in different wells are in resonance, a coherent superposition of distinct states occurs and a gap appears between the energy levels. As a consequence of the coherent quantum tunneling process, in exact resonant conditions, the two levels have an energy tunnel splitting Δ , and the wave functions spread over the two wells, generating delocalized

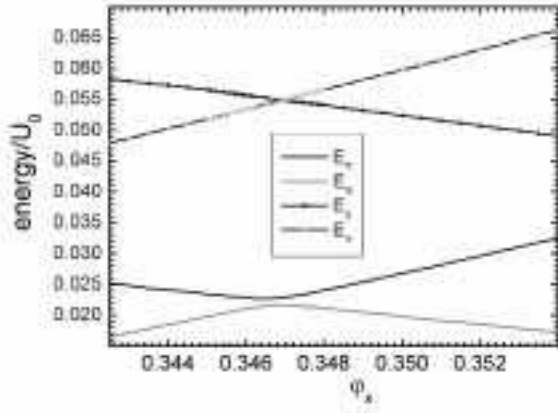


Figure 2. The four essential energy levels considered in this study. All the quantities are referred to the barrier top. Here E_{f_1} and E_{f_2} are the energies of the delocalized levels. E_0 is the first level in the left potential well below E_{f_2} and E_R is the first level in the right potential well below E_{f_2} .

states with energies E_{f_1} and E_{f_2} , as shown in Fig.2. It's worth noting that the energy tunnel splitting Δ corresponds to the tunneling probability T_N in exact resonant conditions and can be experimentally observed only if resonant levels are very close to the barrier top and in small viscosity limit [9].

Moreover, to study the tunneling process from the upper levels, it's necessary to populate them through a pumping process from the ground state of the left well: this requires the application of a microwave irradiation of proper frequency $\nu = \omega/2\pi$ and amplitude \mathcal{I} . Even a small amplitude of external microwave irradiation will cause an essential change in the population of excited states and will therefore produce a large effect in the tunneling probability.

We study the rf-SQUID dynamics in these particular conditions and we show some numerical simulations. For a fixed value of the pumping frequency ν , the transition probability curve W from one potential well to the other one (as a function of the external parameter φ_x) can present three maxima: one maximum is connected with the resonant tunneling and the two others with the resonant pumping toward the two non-localized levels with energies E_{f_1} , E_{f_2} .

In the considered phenomenon, friction, that is due to the interaction with the external environment, has a relevant role since it leads to a finite width γ of levels and destroys the coherence [21]. In the following sections we will discuss the induced resonance phenomena by using the density matrix formalism [22].

In particular in section II we discuss the transition probability function in presence of resonant pumping, in section III we show how to calculate levels position and transition matrix elements, in section IV we determine the energy spectrum in the vicinity of the crossing point and ,finally, in section V we show the results of numerical simulations and first experimental data for the dissipation level for these rf-SQUID based devices.

2. Transition probability function in presence of resonant pumping

In the zero approximation of the system interaction with the thermal bath, the hamiltonian describing the rf-SQUID in the presence of an external microwave with amplitude \mathcal{I} is

$$H_0 = -\frac{\hbar^2}{2M} \frac{\partial^2}{\partial \varphi^2} + U_0 [(\varphi - \varphi_x)^2 + \beta_L \cos \varphi] + \frac{\mathcal{I}\hbar}{2e} \cos(\omega t) \varphi \quad (2)$$

where \mathcal{I} has the dimensionality of a current, M is the “mass” of the Josephson junction defined as

$$M = \left(\frac{\hbar}{2e} \right)^2 C \quad (3)$$

and C is the junction capacitance. Following a common practice[4], the dimensionless variable φ_x is obtained by referring the magnetic flux to $\Phi_0/2$ and normalizing it to $\Phi_0/2\pi$. In eq.(2) quantities U_0 and β_L are free parameters of the system and are defined as

$$U_0 = \left[\left(\frac{\Phi_0}{2\pi} \right)^2 \frac{1}{L} \right] \quad (4)$$

$$\beta_L = \frac{2\pi L I_c}{\Phi_0} \quad (5)$$

L and I_c are the inductance and the critical current of the rf-SQUID, respectively. The simplest case is when U_0 and β_L are constant, while φ_x changes.

Our considerations are valid for any potential $U(\varphi)$. The essential point is that the potential $U(\varphi)$ has the form given in Fig.1 in the proximity of the points $\tilde{\varphi}$. All the parameters φ_x , U_0 , β_L depends on the structure of the considered SQUID.

Here we choose parameters such that, near to the top of the barrier, there are two close levels E_{f_1} , E_{f_2} , that can be considered as belonging to both potential wells simultaneously (delocalized levels) as shown in Fig.1. Moreover it's worth noting that the quantity φ_x is proportional to $\frac{IL}{\Phi_0}$.

The dissipation is accounted for by an effective resistance R_{eff} in the RSJ model for the junction [23]. So a bigger R_{eff} implies a better insulation, that means a smaller width of the levels. Here we consider an rf-SQUID whose Josephson junctions presents a large value of resistance R_{eff} , so that the condition

$$\frac{E_{f_1} - E_{f_2}}{\hbar} \gg \gamma_1, \gamma_2 \quad (6)$$

is satisfied, where γ_1, γ_2 are the widths of levels E_{f_1} , E_{f_2} respectively.

To describe the resonant tunneling induced by the resonant pumping quantitatively, we use the following system of equations [14] for the density matrix elements ρ_f^j

$$\begin{aligned} \frac{\partial \rho_f^j}{\partial t} = & \frac{i\mathcal{I}}{2e} \cos(\omega t) \sum_m \left(\langle j|\varphi|m\rangle \exp \left[-i \left(\frac{E_m - E_j}{\hbar} \right) t \right] \rho_f^m \right. \\ & \left. - \langle m|\varphi|f\rangle \exp \left[i \left(\frac{E_m - E_f}{\hbar} \right) t \right] \rho_m^j \right) + \sum_{m,n} W_{fn}^{jm} \rho_n^m - \frac{1}{2} \sum_m (W_{mj}^{m} + W_{mf}^{m}) \rho_f^j \end{aligned} \quad (7)$$

Here j, m, f, n are the considered levels, E_j, E_m, E_f, E_n are their energies and t is the time.

The matrix elements W_{fn}^{jm} entering in eq.(7) are defined in Appendix A and C. They are nonvanishing provided that

$$|(E_m - E_j) - (E_n - E_f)| \ll \hbar\Omega_p \quad (8)$$

If these conditions are satisfied and if the temperature is low enough, the nonvanishing terms W_{fn}^{jm} of the transition probability matrix are given by the following equation:

$$W_{fn}^{jm} = \frac{\pi}{2R_{eff}e^2} \left(1 + \tanh \frac{\tilde{\omega}}{2T}\right) N(\tilde{\omega}) \cdot \left[\langle j | e^{\frac{i\varphi}{2}} | m \rangle \langle f | e^{-\frac{i\varphi}{2}} | n \rangle + \langle j | e^{-\frac{i\varphi}{2}} | m \rangle \langle f | e^{\frac{i\varphi}{2}} | n \rangle \right] \quad (9)$$

where

$$\tilde{\omega} = \frac{(E_m - E_j + E_n - E_f)}{\hbar} \quad (10)$$

and $N(\tilde{\omega})$ is defined as

$$N(\tilde{\omega}) = \frac{\tilde{\omega}}{\pi} \coth \left(\frac{\tilde{\omega}}{2T} \right) \quad (11)$$

Only the four non-diagonal elements of the density matrix $\rho_{f_1}^0, \rho_{f_2}^0, \rho_0^{f_1}, \rho_0^{f_2}$ are nonzero, and they are connected by the expressions

$$\rho_0^{f_1} = (\rho_{f_1}^0)^* \quad \rho_0^{f_2} = (\rho_{f_2}^0)^* \quad (12)$$

In presence of an external pumping also the two diagonal elements $\rho_{f_1}^{f_1}$ and $\rho_{f_2}^{f_2}$ are nonzero.

We suppose that the temperature T is much smaller than the plasma frequency ($k_B T \ll \hbar\Omega_p$), such that it is of the order of the energy difference $k_B T \approx (E_{f_1} - E_{f_2})$. In the present article we consider $T = 50 \text{ mK}$. When these hypotheses are satisfied, from eq.(7) we obtain

$$\frac{\partial \rho_{f_1}^0}{\partial t} = -\frac{i\mathcal{I}}{2e} \cos(\omega t) \langle 0 | \varphi | f_1 \rangle e^{\left(-i \frac{E_{f_1} - E_0}{\hbar} t\right)} \rho_0^0 + W_{f_1 f_2}^{0 0} \rho_{f_2}^0 - \gamma_1 \rho_{f_1}^0 \quad (13)$$

$$\frac{\partial \rho_{f_2}^0}{\partial t} = -\frac{i\mathcal{I}}{2e} \cos(\omega t) \langle 0 | \varphi | f_2 \rangle e^{\left(-i \frac{E_{f_1} - E_0}{\hbar} t\right)} \rho_0^0 + W_{f_2 f_1}^{0 0} \rho_{f_1}^0 - \gamma_2 \rho_{f_2}^0 \quad (14)$$

where the widths γ_1, γ_2 of levels are given by the following expressions

$$\begin{aligned} \gamma_1 &= \frac{1}{2} \left(W_{f_2 f_1}^{f_2 f_1} + W_{L f_1}^{L f_1} + W_{R f_1}^{R f_1} \right) \\ \gamma_2 &= \frac{1}{2} \left(W_{f_1 f_2}^{f_1 f_2} + W_{L f_2}^{L f_2} + W_{R f_2}^{R f_2} \right) \end{aligned} \quad (15)$$

The indexes L and R refer to the first energy levels below E_{f_2} in the left and right wells, respectively. The tunneling transition probability between two states in different wells decreases very quickly for states below the barrier top, such as $e^{-2\pi n}$, where n is the number of states counted from the barrier top [24]. As a consequence we can neglect transitions into lower levels in the right potential well.

In order to study this phenomenon, only five energy levels ($E_{f_1}, E_{f_2}, E_0, E_L, E_R$) are

essential quantities. E_0 is the energy of the ground state in the left potential well, E_L is the first level in the left potential well below E_{f_2} (in the simulations presented here $E_L=E_0$), E_R is the first level in the right potential well below E_{f_2} . Energy levels as a function of the external parameter φ_x , are shown in Fig.2. The pumping frequency ν is supposed to be close to the frequencies E_{f_1}/\hbar and E_{f_2}/\hbar (referring both to E_0/\hbar). In our simulations E_L is also the ground state of the left potential well (it's the same as E_0), while in the right well there are many more levels, not involved in the described process.

If these conditions are satisfied, the solutions of eqs.(13), (13) are:

$$\begin{aligned}\rho_{f_1}^0 &= A_{f_1} e^{i\left(\omega - \frac{E_{f_1}-E_0}{\hbar}\right)t} + B_{f_1} e^{i\left(\omega - \frac{E_{f_2}-E_0}{\hbar}\right)t} \\ \rho_{f_2}^0 &= B_{f_2} e^{i\left(\omega - \frac{E_{f_1}-E_0}{\hbar}\right)t} + A_{f_2} e^{i\left(\omega - \frac{E_{f_2}-E_0}{\hbar}\right)t}\end{aligned}\quad (16)$$

In eqs.(16) coefficients A_{f_1} , A_{f_2} , B_{f_1} , B_{f_2} are defined as follows

$$\begin{aligned}A_{f_1} &= -\frac{\mathcal{I}}{4e} \langle 0|\varphi|f_1\rangle \left[\omega - \frac{E_{f_1}-E_0}{\hbar} - i\gamma_1 + \frac{W_{f_1 f_2}^{00} W_{f_2 f_1}^{00}}{\omega - \frac{E_{f_1}-E_0}{\hbar} - i\gamma_2} \right]^{-1} \\ A_{f_2} &= -\frac{\mathcal{I}}{4e} \langle 0|\varphi|f_2\rangle \left[\omega - \frac{E_{f_2}-E_0}{\hbar} - i\gamma_2 + \frac{W_{f_1 f_2}^{00} W_{f_2 f_1}^{00}}{\omega - \frac{E_{f_2}-E_0}{\hbar} - i\gamma_1} \right]^{-1} \\ B_{f_1} &= -\frac{iW_{f_1 f_2}^{00} A_{f_2}}{\omega - \frac{E_{f_2}-E_0}{\hbar} - i\gamma_1} \\ B_{f_2} &= -\frac{iW_{f_2 f_1}^{00} A_{f_1}}{\omega - \frac{E_{f_1}-E_0}{\hbar} - i\gamma_2}\end{aligned}\quad (17)$$

The diagonal elements $\rho_{f_1}^{f_1}$ and $\rho_{f_2}^{f_2}$ of the density matrix can be find by solving the following equations

$$\begin{aligned}\frac{\partial \rho_{f_1}^{f_1}}{\partial t} &= \frac{i\mathcal{I}}{2e} \cos(\omega t) \left[\rho_{f_1}^0 \langle f_1|\varphi|0\rangle e^{i\left(\frac{E_{f_1}-E_0}{\hbar}\right)t} - \rho_0^{f_1} \langle 0|\varphi|f_1\rangle e^{-i\left(\frac{E_{f_1}-E_0}{\hbar}\right)t} \right] + W_{f_1 f_2}^{f_1 f_2} \rho_{f_2}^{f_2} - 2\gamma_{f_1} \rho_{f_1}^{f_1} \\ \frac{\partial \rho_{f_2}^{f_2}}{\partial t} &= \frac{i\mathcal{I}}{2e} \cos(\omega t) \left[\rho_{f_2}^0 \langle f_2|\varphi|0\rangle e^{i\left(\frac{E_{f_2}-E_0}{\hbar}\right)t} - \rho_0^{f_2} \langle 0|\varphi|f_2\rangle e^{-i\left(\frac{E_{f_2}-E_0}{\hbar}\right)t} \right] + W_{f_2 f_1}^{f_2 f_1} \rho_{f_1}^{f_1} - 2\gamma_{f_2} \rho_{f_2}^{f_2}\end{aligned}\quad (18)$$

These rate equations completely describe the dynamics of the process. The solutions of this system are respectively:

$$\rho_{f_1}^{f_1}(t) = \hat{\rho}_{f_1}^{f_1} + \mathcal{F}_1 e^{i\left(\frac{E_{f_2}-E_{f_1}}{\hbar}\right)t} + \mathcal{F}_1^* e^{-i\left(\frac{E_{f_2}-E_{f_1}}{\hbar}\right)t} \quad (20)$$

$$\rho_{f_2}^{f_2}(t) = \hat{\rho}_{f_2}^{f_2} + \mathcal{D}_1 e^{i\left(\frac{E_{f_2}-E_{f_1}}{\hbar}\right)t} + \mathcal{D}_1^* e^{-i\left(\frac{E_{f_2}-E_{f_1}}{\hbar}\right)t} \quad (21)$$

The expressions for \mathcal{F}_1 and \mathcal{D}_1 are given in Appendix A. By using equations (20) and (21) inside equations (18) and (19), we obtain the expressions of the quantities $\hat{\rho}_{f_1}^{f_1}$ and $\hat{\rho}_{f_2}^{f_2}$ as following:

$$\hat{\rho}_{f_1}^{f_1} = \frac{\mathcal{I}^2}{16e^2} \frac{1}{\gamma_1 \gamma_2 - \frac{1}{4} W_{f_2 f_1}^{f_2 f_1} W_{f_1 f_2}^{f_1 f_2}}$$

$$\begin{aligned}
 & \cdot \left[\gamma_2 | \langle 0 | \varphi | f_1 \rangle |^2 \frac{\gamma_1 - \gamma_2 W_{f_1 f_2}^{00} W_{f_2 f_1}^{00} \left[\left(\omega - \frac{E_{f_1} - E_0}{\hbar} \right)^2 + \gamma_2^2 \right]^{-1}}{\left(\omega - \frac{E_{f_1} - E_0}{\hbar} \right)^2 + \gamma_1^2 + \frac{(W_{f_1 f_2}^{00} W_{f_2 f_1}^{00})^2 + 2W_{f_1 f_2}^{00} W_{f_2 f_1}^{00} \left[\left(\omega - \frac{E_{f_1} - E_0}{\hbar} \right)^2 - \gamma_1 \gamma_2 \right]}{\left(\omega - \frac{E_{f_1} - E_0}{\hbar} \right)^2 + \gamma_2^2}} \right. \\
 & + \frac{1}{2} W_{f_1 f_2}^{f_1 f_2} | \langle 0 | \varphi | f_2 \rangle |^2 \frac{\gamma_2 - \gamma_1 W_{f_1 f_2}^{00} W_{f_2 f_1}^{00} \left[\left(\omega - \frac{E_{f_2} - E_0}{\hbar} \right)^2 + \gamma_1^2 \right]^{-1}}{\left(\omega - \frac{E_{f_2} - E_0}{\hbar} \right)^2 + \gamma_2^2 + \frac{(W_{f_1 f_2}^{00} W_{f_2 f_1}^{00})^2 + 2W_{f_1 f_2}^{00} W_{f_2 f_1}^{00} \left[\left(\omega - \frac{E_{f_2} - E_0}{\hbar} \right)^2 - \gamma_1 \gamma_2 \right]}{\left(\omega - \frac{E_{f_2} - E_0}{\hbar} \right)^2 + \gamma_1^2}} \left. \right] \quad (22)
 \end{aligned}$$

$$\begin{aligned}
 \hat{\rho}_{f_2}^{f_2} &= \frac{\mathcal{I}^2}{16e^2} \frac{1}{\gamma_1 \gamma_2 - \frac{1}{4} W_{f_2 f_1}^{f_2 f_1} W_{f_1 f_2}^{f_1 f_2}} \\
 & \cdot \left[\gamma_1 | \langle 0 | \varphi | f_2 \rangle |^2 \frac{\gamma_2 - \gamma_1 W_{f_2 f_1}^{00} W_{f_1 f_2}^{00} \left[\left(\omega - \frac{E_{f_2} - E_0}{\hbar} \right)^2 + \gamma_1^2 \right]^{-1}}{\left(\omega - \frac{E_{f_2} - E_0}{\hbar} \right)^2 + \gamma_2^2 + \frac{(W_{f_1 f_2}^{00} W_{f_2 f_1}^{00})^2 + 2W_{f_1 f_2}^{00} W_{f_2 f_1}^{00} \left[\left(\omega - \frac{E_{f_2} - E_0}{\hbar} \right)^2 - \gamma_1 \gamma_2 \right]}{\left(\omega - \frac{E_{f_2} - E_0}{\hbar} \right)^2 + \gamma_1^2}} \right. \\
 & + \frac{1}{2} W_{f_2 f_1}^{f_2 f_1} | \langle 0 | \varphi | f_1 \rangle |^2 \frac{\gamma_1 - \gamma_2 W_{f_1 f_2}^{00} W_{f_2 f_1}^{00} \left[\left(\omega - \frac{E_{f_1} - E_0}{\hbar} \right)^2 + \gamma_2^2 \right]^{-1}}{\left(\omega - \frac{E_{f_1} - E_0}{\hbar} \right)^2 + \gamma_1^2 + \frac{(W_{f_1 f_2}^{00} W_{f_2 f_1}^{00})^2 + 2W_{f_1 f_2}^{00} W_{f_2 f_1}^{00} \left[\left(\omega - \frac{E_{f_1} - E_0}{\hbar} \right)^2 - \gamma_1 \gamma_2 \right]}{\left(\omega - \frac{E_{f_1} - E_0}{\hbar} \right)^2 + \gamma_2^2}} \left. \right] \quad (23)
 \end{aligned}$$

Finally we can introduce the transition probability W from the left to the right potential well. W is a function of the external parameter φ_x and computing this quantity is the main goal of the paper. The transition probability is given by the expression

$$W = W_{R f_1}^{R f_1} \rho_{f_1}^{f_1} + W_{R f_2}^{R f_2} \rho_{f_2}^{f_2} \quad (24)$$

where, in the low temperature limit, here considered, from eq.(9) we know that

$$W_{R f_1}^{R f_1} = \frac{2(E_{f_1} - E_R)}{R_{eff} e^2} | \langle R | e^{i\varphi/2} | f_1 \rangle |^2 \quad (25)$$

$$W_{R f_2}^{R f_2} = \frac{2(E_{f_2} - E_R)}{R_{eff} e^2} | \langle R | e^{i\varphi/2} | f_2 \rangle |^2 \quad (26)$$

while the expressions for $\rho_{f_1}^{f_1}$ and $\rho_{f_2}^{f_2}$ are given in eqs.(20) and (21) respectively. In the eqs. (22) and (23), the quantities \mathcal{F}_1 and \mathcal{D}_1 determinate the value of the oscillating part of the tunneling probability W .

It's worth noting that change of the external parameter φ_x leads to a redistribution of wave functions relative to energies E_{f_1} , E_{f_2} between left and right potential wells, so that transition matrix elements and widths of levels γ_1 , γ_2 are functions of the external parameter φ_x . To complete our considerations we will find the levels position and the transition matrix elements as a function of the external parameters, as shown in the

3. Levels position and transition matrix elements.

As we have seen before, a necessary condition for resolving the splitting is that the experimental linewidth of states (γ_1, γ_2) be smaller than Δ ($\Delta \gg \hbar\gamma_1, \hbar\gamma_2$): it can be satisfied only for levels near to the barrier top (Fig.1). In Fig.1 $\varphi_1, \varphi_2, \varphi_3, \varphi_4$ are the “turning points”, that are the solutions of equation

$$U(\varphi_{1,2,3,4}) = E \quad (27)$$

where E is the energy value. In Fig.1 the points $\varphi_1^{min}, \varphi_2^{min}$ are coordinates corresponding to the minima of potential $U(\varphi)$ and the point φ_{top} is the coordinate corresponding to the maximum of the potential $U(\varphi)$. For energy values E close to the top of the barrier, the wave function Ψ can be written in the form

$$\Psi = G^{-1} \cdot \frac{1}{(2M(E - U(\varphi)))^{1/4}} \sin \left(\frac{\pi}{4} + \int_{\varphi_1} \sqrt{2M(E - U(\varphi))} d\varphi \right) \text{ in the left potential well}$$

$$\Psi = A \cdot \mathcal{D}_{-\frac{1-i\lambda}{2}}((1+i)(2MU_1)^{1/4}(\varphi - \varphi_{top})) + A^* \mathcal{D}_{-\frac{1+i\lambda}{2}}((1-i)(2MU_1)^{1/4}(\varphi - \varphi_{top})) \text{ near the barrier top} \quad (28)$$

$$\Psi = \frac{B}{(2M(E - U(\varphi)))^{1/4}} \sin \left(\frac{\pi}{4} + \int^{\varphi_4} \sqrt{2M(E - U(\varphi))} d\varphi \right) \text{ in the right potential well}$$

In eqs.(28) \mathcal{D}_p is the parabolic cylinder function [25], while quantities A and B are numerical factors, G is a normalization factor, defined in the following. The other quantities are defined as

$$U_{top} = U(\varphi_{top}) \quad (29)$$

$$U_1 = -\frac{1}{2} \left(\frac{\partial^2 U}{\partial \varphi^2} \right)_{\varphi=\varphi_{top}} \quad (30)$$

$$\lambda = \sqrt{2MU_1} \frac{U_{top} - E}{U_1} \quad (31)$$

First expression in eqs.(28) is valid in the left potential well, the second one is valid close to the barrier top, the third one is valid in the right potential well. Coefficients A, B are defined by imposing boundary conditions for these three expressions. Near to the top of the potential barrier we use the exact solutions of the Schroedinger equation for the considered system, whereas in the vicinity of the points φ_1, φ_4 we use the well note method of outgoing in complex plane[26]. The relation between coefficients A and B can be found by matching coefficients in the right potential well

$$A = \frac{B}{2^{3/4}(2MU_1)^{1/8}} \exp \left[\frac{\pi\lambda}{8} - \frac{i\pi}{8} + \frac{i\lambda}{4} + \frac{i\lambda}{4} \ln \left(\frac{2}{\lambda} \right) + i \int_{\varphi_3}^{\varphi_4} d\varphi \sqrt{2M(E - U(\varphi))} \right] \quad (32)$$

By matching boundary conditions in the left potential we obtain two equations. The first one is the exact equation for the position of the levels near the barrier top in the case of small viscosity limit

$$\cos \left(\int_{\varphi_3}^{\varphi_4} d\varphi \sqrt{2M(E - U(\varphi))} - \int_{\varphi_1}^{\varphi_2} d\varphi \sqrt{2M(E - U(\varphi))} \right) + (1 + \exp(-\pi\lambda))^{1/2} \cdot \cos \left(\chi + \frac{\lambda}{2} + \frac{\lambda}{2} \ln \left(\frac{2}{\lambda} \right) + \int_{\varphi_3}^{\varphi_4} d\varphi \sqrt{2M(E - U(\varphi))} + \int_{\varphi_1}^{\varphi_2} d\varphi \sqrt{2M(E - U(\varphi))} \right) = 0 \quad (33)$$

In eq.(33) phase shift χ is defined by the expression

$$\Gamma \left(\frac{1 + i\lambda}{2} \right) = \frac{\sqrt{2\pi} e^{(-\pi\lambda/4)}}{\sqrt{1 + e^{(-\pi\lambda)}}} e^{(i\chi)} \quad (34)$$

where $\Gamma(x)$ is the Euler gamma function and the phase χ can be presented in the form

$$\chi = \frac{\lambda}{2} \Psi \left(\frac{1}{2} \right) - \sum_{k=0}^{\infty} \left(\arctan \left(\frac{\lambda}{2k+1} \right) - \frac{\lambda}{2k+1} \right) \quad (35)$$

In eq.(35) $\psi(x)$ is the Euler function and

$$\psi \left(\frac{1}{2} \right) = -C - 2 \ln 2 = -1.96351$$

The second equation gives the value of the coefficient B as follows

$$B = \exp \left(\frac{\pi\lambda}{2} \right) \left[(1 + \exp(-\pi\lambda))^{1/2} \sin \left(\chi + \frac{\lambda}{2} + \frac{\lambda}{2} \ln \left(\frac{2}{\lambda} \right) + \int_{\varphi_1}^{\varphi_2} d\varphi \sqrt{2M(E - U(\varphi))} + \int_{\varphi_3}^{\varphi_4} d\varphi \sqrt{2M(E - U(\varphi))} - \sin \left(\int_{\varphi_1}^{\varphi_2} d\varphi \sqrt{2M(E - U(\varphi))} - \int_{\varphi_3}^{\varphi_4} d\varphi \sqrt{2M(E - U(\varphi))} \right) \right]$$

In order to obtain two close levels near to the barrier top (but not too close) the parameter λ should be $\lambda \geq 1$. In such a case, the normalization factor G can be approximated as

$$G^2 = \frac{\hbar}{2} \left(\int_{\varphi_1}^{\varphi_2} \frac{d\varphi}{\sqrt{2M(E - U(\varphi))}} + B^2 \int_{\varphi_3}^{\varphi_4} \frac{d\varphi}{\sqrt{2M(E - U(\varphi))}} \right) \quad (37)$$

Since we consider the energy E close to the barrier top, it's possible to use expressions with explicit energy dependence (perturbation theory over the quantity $(U_{top} - E)$ with separation of the singular terms):

$$\int_{\varphi_1}^{\varphi_2} d\varphi \sqrt{2M(E - U(\varphi))} = \int_{\tilde{\varphi}_1}^{\varphi_{top}} d\varphi \sqrt{2M(U_{top} - U(\varphi))} - (U_{top} - E) \sqrt{\frac{M}{2}} \int_{\tilde{\varphi}_1}^{\varphi_{top}} d\varphi \left(\frac{1}{\sqrt{(U_{top} - U(\varphi))}} - (U_{top} - E) \sqrt{\frac{M}{2U_1}} \left[\ln \left(\frac{8(\varphi_{top} - \tilde{\varphi}_1) \sqrt{U_1}}{\sqrt{U_{top} - E}} \right) + \frac{1}{2} \right] \right]$$

$$\int_{\varphi_3}^{\varphi_4} d\varphi \sqrt{2M(E - U(\varphi))} = \int_{\varphi_{top}}^{\tilde{\varphi}_4} d\varphi \sqrt{2M(U_{top} - U(\varphi))} - (U_{top} - E) \sqrt{\frac{M}{2}} \int_{\varphi_{top}}^{\tilde{\varphi}_4} d\varphi \left(\frac{1}{\sqrt{(U_{top} - U(\varphi))}} - \frac{1}{\sqrt{(U_{top} - E)}} \right) - (U_{top} - E) \sqrt{\frac{M}{2U_1}} \left[\ln \left(\frac{8(\tilde{\varphi}_4 - \varphi_{top}) \sqrt{U_1}}{\sqrt{U_{top} - E}} \right) + \frac{1}{2} \right]$$

In eqs.(38), (39) quantities $\tilde{\varphi}_1$, $\tilde{\varphi}_4$ are defined as

$$\tilde{\varphi}_1 = \varphi_1 (E = U_{top})$$

$$\tilde{\varphi}_4 = \varphi_4 (E = U_{top})$$

Energies E_L , E_R of states Ψ_L , Ψ_R can be found by using eqs.(33), (38), (39), provided that Ψ_L , Ψ_R are referred to the barrier top. In this case wavefunctions Ψ_L , Ψ_R can be described by using the quasiclassical approximation, so that we find

$$\Psi_L = \frac{1}{G_L} \frac{\sin \left(\frac{\pi}{4} + \int_{\varphi_1}^{\varphi} d\varphi \sqrt{2M(E - U(\varphi))} \right)}{(2M(E - U(\varphi)))^{1/4}} \quad (40)$$

$$\Psi_R = \frac{1}{G_R} \frac{\sin \left(\frac{\pi}{4} + \int_{\varphi}^{\varphi_4} d\varphi \sqrt{2M(E - U(\varphi))} \right)}{(2M(E - U(\varphi)))^{1/4}} \quad (41)$$

where the factors G_L and G_R are defined as

$$G_L^2 = \frac{\hbar}{2} \int_{\varphi_1}^{\varphi_2} \frac{d\varphi}{\sqrt{2M(E - U(\varphi))}} \quad (42)$$

$$G_R^2 = \frac{\hbar}{2} \int_{\varphi_3}^{\varphi_4} \frac{d\varphi}{\sqrt{2M(E - U(\varphi))}} \quad (43)$$

The wave function Ψ_0 of the ground state can be taken in the form

$$\Psi_0 = \frac{(2MU_1^{min})^{1/8}}{\pi^{1/4}} e^{-\int_{\varphi_1^{min}}^{\varphi} d\varphi \sqrt{2M(U(\varphi) - U(\varphi_1^{min}))}} \quad (44)$$

where $U_{1,2}^{min} = U(\varphi_{1,2}^{min})$ and $\varphi_{1,2}^{min}$ are the coordinates corresponding to the position of the left and right minimum in the potential $U(\varphi)$

$$\left(\frac{\partial U}{\partial \varphi} \right)_{\varphi=\varphi_{1,2}^{min}} = 0$$

$$U(\varphi) = U(\varphi_{1,2}^{min}) + U_{1,2}^{min}(\varphi - \varphi_{1,2}^{min})^2 + \dots$$

4. The energy spectrum in the vicinity of the crossing point.

In order to describe the spectrum near to the crossing point we introduce two functions Φ_1 and Φ_2 , defined as:

$$\Phi_1 = \int_{\varphi_1}^{\varphi_2} d\varphi \sqrt{2M(E - U(\varphi))} + \frac{\lambda}{4} \left(1 + \ln \left(\frac{2}{\lambda} \right) \right) = \int_{\tilde{\varphi}_1}^{\varphi_{top}} d\varphi \sqrt{2M(U_{top} - U(\varphi))}$$

$$\begin{aligned}
 & - (U_{top} - E) \sqrt{\frac{M}{2}} \int_{\tilde{\varphi}_1}^{\varphi_{top}} d\varphi \left(\frac{1}{\sqrt{U_{top} - U(\varphi)}} - \frac{\sqrt{\varphi_{top} - \tilde{\varphi}_1}}{(\varphi_{top} - \varphi) \left(\sqrt{U_1(\varphi - \tilde{\varphi}_1)} \right)} \right) \\
 & + (U_{top} - E) \sqrt{\frac{M}{2U_1}} \ln \left(\frac{2^{1/4}}{8 (MU_1)^{1/4} (\varphi_{top} - \tilde{\varphi}_1)} \right)
 \end{aligned} \tag{45}$$

$$\begin{aligned}
 \Phi_2 &= \int_{\varphi_3}^{\varphi_4} d\varphi \sqrt{2M(E - U(\varphi))} + \frac{\lambda}{4} \left(1 + \ln \left(\frac{2}{\lambda} \right) \right) = \int_{\varphi_{top}}^{\tilde{\varphi}_4} d\varphi \sqrt{2M(U_{top} - U(\varphi))} \\
 & - (U_{top} - E) \sqrt{\frac{M}{2}} \int_{\varphi_{top}}^{\tilde{\varphi}_4} d\varphi \left(\frac{1}{\sqrt{U_{top} - U(\varphi)}} - \frac{\sqrt{\tilde{\varphi}_4 - \varphi_{top}}}{(\varphi - \varphi_{top}) \left(\sqrt{U_1(\tilde{\varphi}_4 - \varphi)} \right)} \right) \\
 & + (U_{top} - E) \sqrt{\frac{M}{2U_1}} \ln \left(\frac{2^{1/4}}{8 (MU_1)^{1/4} (\tilde{\varphi}_4 - \varphi_{top})} \right)
 \end{aligned} \tag{46}$$

Now, we suppose that for some value of the external parameters $\varphi_x^0, U_0, \beta_L$ there is a point characterized by $E_0, \lambda_0 = \lambda(E_0)$ (defined in eq.31) such that

$$\Phi_1(U_0, \beta_L, \varphi_x^0, E_0, \lambda_0) + \frac{1}{2}\chi(\lambda_0) = \frac{\pi}{2} + \pi k_1 \tag{47}$$

$$\Phi_2(U_0, \beta_L, \varphi_x^0, E_0, \lambda_0) + \frac{1}{2}\chi(\lambda_0) = \frac{\pi}{2} + \pi k_2 \tag{48}$$

where k_1, k_2 are integer numbers. The equations (46),(47) determine the "crossing point". In fact, we are interested to find the external parameter φ_x such that the two energy levels E_{f1} and E_{f2} are close. As a consequence, next to this special point, we can use Taylor expansion for the functions Φ_1 and Φ_2 and we can write:

$$\Phi_1 + \frac{1}{2}\chi = \frac{\pi}{2} + \pi k_1 + \alpha_1 \delta\varphi_x + \beta_1 \delta E \tag{49}$$

$$\Phi_2 + \frac{1}{2}\chi = \frac{\pi}{2} + \pi k_2 + \alpha_2 \delta\varphi_x + \beta_2 \delta E \tag{50}$$

where

$$E = E_0 + \delta E, \quad \varphi_x = \varphi_x^0 + \delta\varphi_x \tag{51}$$

and the quantities $\alpha_1, \alpha_2, \beta_1, \beta_2$ can be found from eqs.(2), (45). They are given in Appendix B. From eqs.(33), (49), (50) we obtain the equation to calculate the energy spectrum for two close levels near to the barrier top

$$\begin{aligned}
 & \beta_1 \beta_2 (\delta E)^2 + \alpha_1 \alpha_2 (\delta\varphi_x)^2 \\
 & + (\alpha_1 \beta_2 + \alpha_2 \beta_1) \delta\varphi_x \delta E - \frac{1}{4} e^{(-\pi\lambda)} = 0
 \end{aligned} \tag{52}$$

The solutions of this equation are two hyperboles

$$\delta E = -\frac{1}{2\beta_1 \beta_2} \left[(\alpha_1 \beta_2 + \alpha_2 \beta_1) \delta\varphi_x \pm \sqrt{(\alpha_1 \beta_2 - \alpha_2 \beta_1)^2 (\delta\varphi_x)^2 + \beta_1 \beta_2 \exp(-\pi\lambda)} \right] \tag{53}$$

Note that Eq.53 gives the position of two close levels as function of the external parameter φ_x . Two levels can be defined close if $\delta E \ll \hbar\Omega_p$ (the plasma frequency, defined

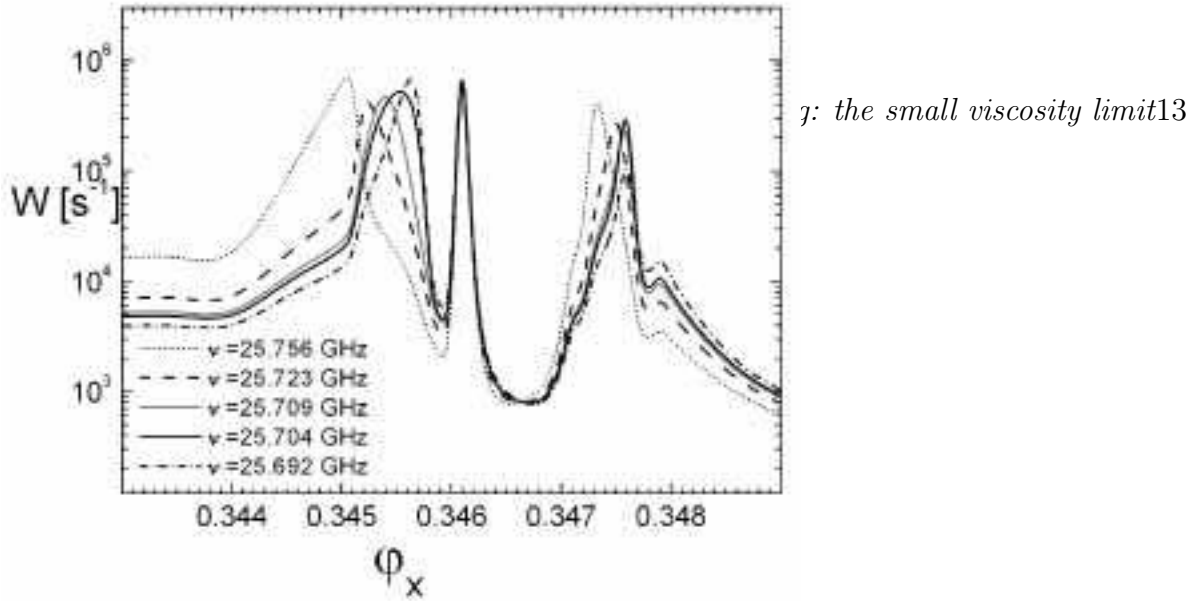


Figure 3. Transition probability W vs. φ_x for different values of the pumping frequency ν . W presents three peaks: the central one is due to the resonance tunneling and two lateral ones are due to the resonant pumping of the two levels close to the barrier top. Curves are obtained by using the following parameters for the numerical simulation: $\beta_L=1.75$, $L=210$ pH, $C=0.1$ pF, and $R_{eff}=8$ M Ω .

in the introduction) and this occurs if the parameter $\exp(-\pi\lambda)$ is small, that is if λ is of the order of one.

5. Numerical simulations and preliminary measurements

In this section we suggest a set of SQUID parameters useful in order to observe experimentally the effect here studied with this new theoretical approach. The experiment can be realized by following the experimental scheme described in [8]. The external parameter φ_x biasing the rf-SQUID is varied as a function of the time until a switching from one fluxoid state to another one is observed. The statistical distribution of the switching value φ_x can be measured by repeating the process many times (about 10^4 measurements). From the switching value distribution is straightforward to obtain the escape rate W and compare data and theory. The first significant comparison is then the dependence of the escape rate as a function of φ_x , showing the characteristic peaks due to ELQ and MQC phenomena. For these simulations we consider a temperature $T=50$ mK and some reasonable rf-SQUID parameters, as: $\beta_L=1.75$, $L=210$ pH, $C=0.1$ pF, and $R_{eff}=8$ M Ω .

In the extremely underdamped limit, the number of peaks of the transition probability W vs. φ_x , can be three or one depending on the pumping frequency value ν .

In the three peaks curves (Fig.3), the central peak is always connected with the resonant tunneling, while the two other peaks are connected with the resonant pumping. The central peak is due to the coherent tunneling between levels f_1 and f_2 . As a consequence, it's fixed in position and height, even if we change the frequency ν , since it is

correlated to the anticrossing point, that does not depend on the external irradiation. On the contrary, the other two peaks have a shift depending on the frequency. The left side peak corresponds to a transition from the ground state in the left well to the state f_1 , while the right side peak is connected to the transition from the ground state to the state f_2 . Of course these transitions occur at values of the external flux φ_x which depend on the pumping frequency, as shown in Fig.4. Infact, if we represent the external field

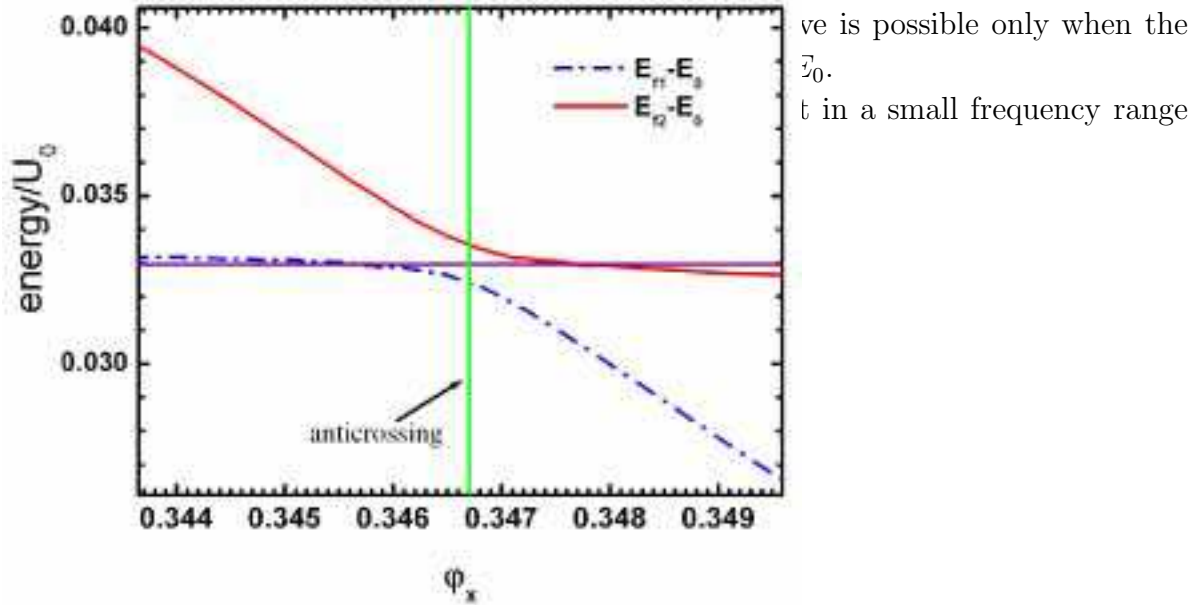


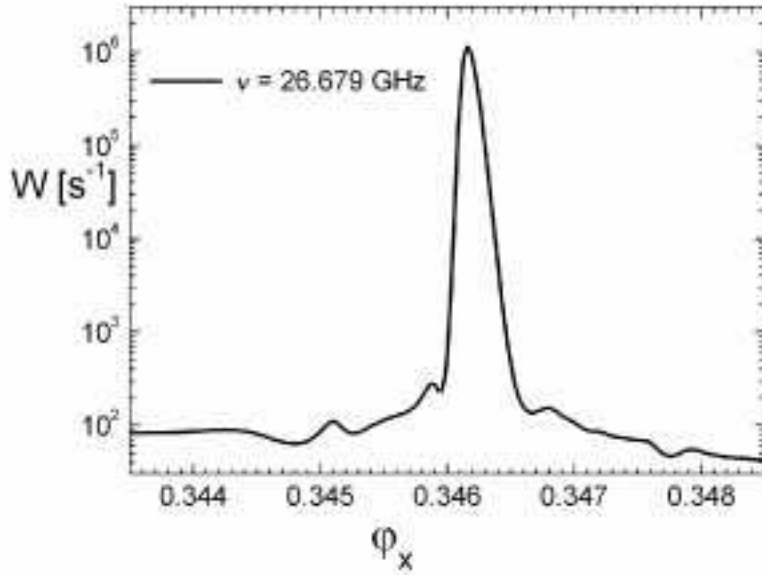
Figure 4. Curves $E_{f_1} - E_0$ vs. φ_x and $E_{f_2} - E_0$ vs. φ_x . All the energies are referred to the barrier top. The horizontal line is the external field of frequency ν , it crosses the energy curves $E_{f_1} - E_0$ and $E_{f_2} - E_0$ in two points. The vertical line represents the coordinate corresponding to the anticrossing point. Comparison of Figs.3 -4 shows that the first peak correspond to the resonant pumping from the ground state in the left well to the state with energy E_{f_1} while the third peak corresponds to the resonant pumping from the ground state from the ground state to the state with energy E_{f_2} . For all the parameters values are: $\beta_L = 1.75$, $C = 0.1$ pF, $L = 210$ pH.

around the anticrossing point. For all other frequencies we find the one peak curve (Fig.5), where the only peak is due to the resonant tunneling.

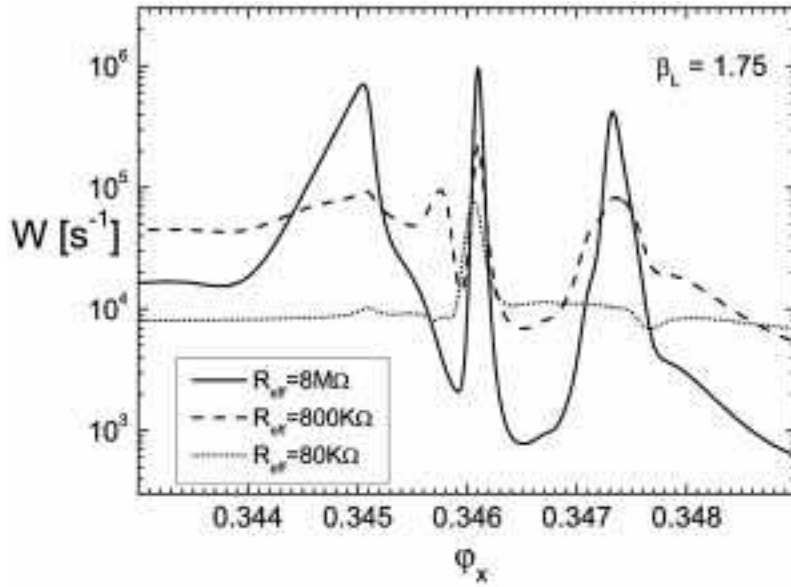
For these simulations we have considered pumping frequencies ranging from $\nu = \omega/2\pi = 25.6$ GHz to $\nu = 26.8$ GHz. These values assure that the excited pumped level in the left potential well is close to some level in right potential well.

Moreover it is interesting to study the dependence of the peaks on the effective dissipation described in the RSJ model by the effective resistance R_{eff} , and this is shown in Fig.6. As expected [27], by decreasing dissipation, that is by increasing R_{eff} , peaks resolution is enhanced.

Also the β_L parameter can be varied in the experiments [9] and therefore we present some numerical simulations to study the transition probability W vs. φ_x for two different β_L values (see fig.7, fig.8 and fig.9). It's worth noting that to vary β_L for the rf-SQUID, we vary only the value of the inductance L (see eq.4) and a variation of β_L corresponds



γ : the small viscosity limit 15



he W presents only one peak due
y using the following parameters
 $C=0.1$ pF, and $R_{eff}=8$ MΩ.

Figure 6. Transition probability W vs. φ_x for different values of the effective resistance R_{eff} . The plot was obtained by using the following parameters for the numerical simulation: $\beta_L=1.75$, $L=210$ pH, $C=0.1$ pF, $\nu= 25.756$ GHz.

to the variation of the height of the potential barrier. We stress that, when we increase the β_L value, the transition probability becomes smaller and we need to increase the external parameter to observe the peaks.

Finally we also made a study of the dependence of the peaks distribution and behavior on the capacitance C . We observed that by decreasing the C value, the peaks in the transition probability become higher and more enhanced.

The best set of values for these parameters is when the β_L and the capacitance C values are not too large.

The predicted process can be observed by escape rate measurements. Since we want study Macroscopic Quantum Phenomena, we projected and realized devices with a low

Figure 7. Transition probability W vs. φ_x for $\beta_L=2.15$, $L=258$ pH, $C=0.1$ pF, $R_{eff}=8$ M Ω and $\nu=32.818$ GHz.

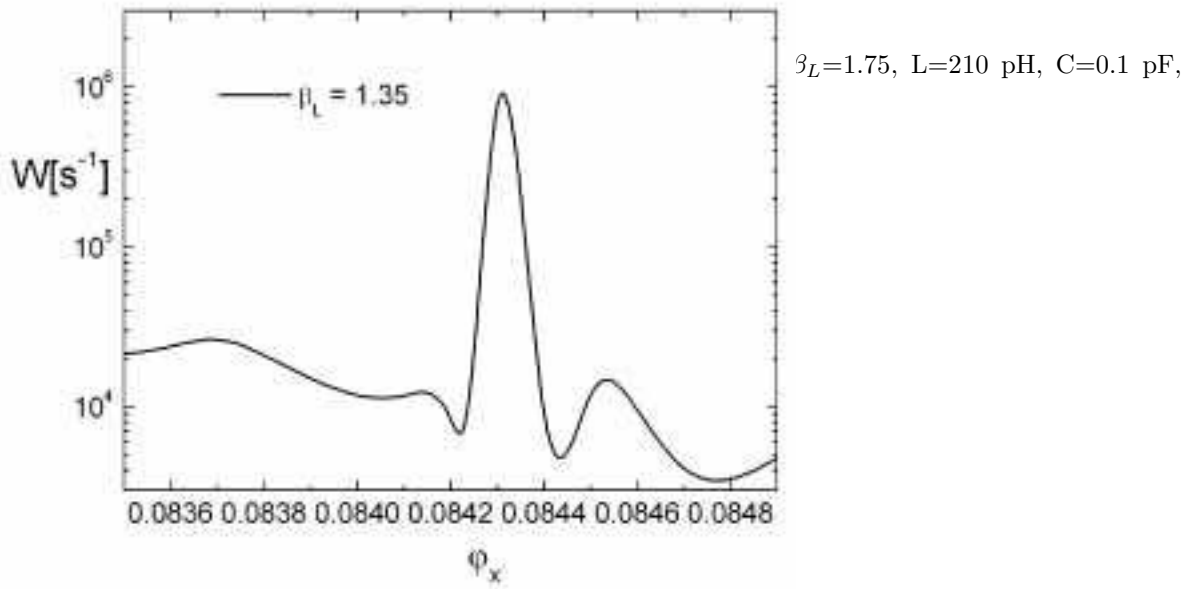


Figure 9. Transition probability W vs. φ_x for $\beta_L=1.35$, $L=162$ pH, $C=0.1$ pF, $R_{eff}=8$ M Ω and $\nu=24.456$ GHz.

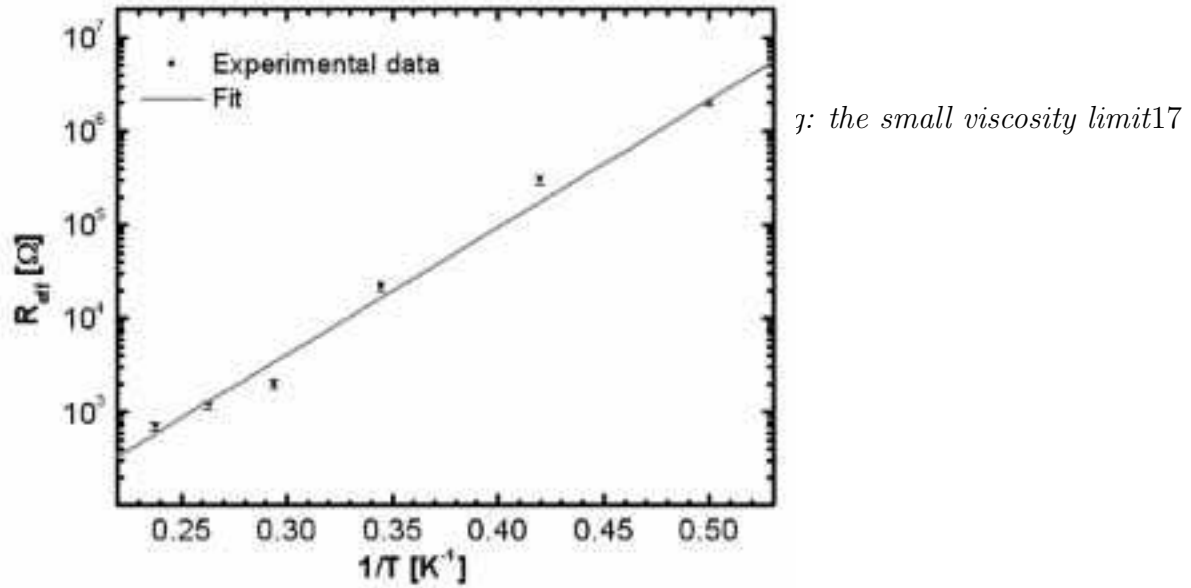


Figure 10. Dots are experimental data for R_{eff} in our devices at different temperatures, while the line is the linear fit, corresponding to the expression $R_{eff} = R_0 \exp(\Delta/k_B T)$.

dissipation level. The preliminary measurements on our devices have confirmed a really low dissipation level [5], with a really high effective resistance, as shown in Fig.10. These results indicate that our devices are good candidates for quantum measurements.

6. Conclusions

The results presented here describe the small viscosity limit in the problem of resonant quantum tunneling for an rf-SQUID, whose parameters can be determined with independent measurements. All the physical quantities here considered are very sensitive to the external parameters.

It's worth noting that we considered levels below the top of the classical energy barrier. This condition is essential, since in this case the levels (in the absence of coherence) can be exclusively associated with one well and moreover it's a necessary condition in order to observe tunneling phenomena.

The transition probability function W from the left potential well to the right one has been calculated by varying φ_x and for different values of the pumping frequency ν , of the β_L parameter and for different values of the effective resistance R_{eff} . The results obtained here suggest that the resonant quantum tunneling is a convenient tool for investigating macroscopic quantum coherence phenomena.

The dependence of the transition probability W on the external parameter φ_x shows three peaks (Fig.3). The first is connected with the resonant tunneling and the others two are associated with the resonant pumping toward the two non-localized energy levels. The relative positions of these two peaks strictly depend on the pumping frequency and on the external parameter biasing the rf-SQUID. Moreover the transition probability W is obtained as a function of the potential parameters and of the shunt resistance R_{eff} . Preliminary experimental measurements on our devices confirmed a low dissipation level [5], with a high effective resistance, as shown in Fig.10. These results, albeit

still unconfirmed by a wider and more accurate experimental campaign, would suggest potential for interesting observations regarding the resonant phenomena in the presence of an external microwave irradiation of proper frequency.

Appendix A.

From eqs.(7), (13) we obtain two equations depending on the quantities \mathcal{D}_1 and \mathcal{F}_1

$$\begin{aligned} \mathcal{F}_1 \left[\left(\frac{E_{f_2} - E_{f_1}}{\hbar} \right) - 2i\gamma_1 \right] + iW_{f_1 f_2}^{f_1 f_2} \mathcal{D}_1 &= \frac{i\mathcal{I}^2}{16e^2} \cdot \left[\frac{\langle 0|\varphi|f_1\rangle\langle f_2|\varphi|0\rangle W_{f_1 f_2}^{0 0}}{\left(\omega - \left(\frac{E_{f_2} - E_0}{\hbar} \right) \right)^2 - \gamma_1\gamma_2 + W_{f_1 f_2}^{0 0} W_{f_2 f_1}^{0 0} + i(\gamma_1 + \gamma_2) \left(\omega - \frac{E_{f_2} - E_0}{\hbar} \right)} \right. \\ iW_{f_2 f_1}^{f_2 f_1} \mathcal{F}_1 + \mathcal{D}_1 \left[\left(\frac{E_{f_2} - E_{f_1}}{\hbar} \right) - 2i\gamma_2 \right] &= \frac{i\mathcal{I}^2}{16e^2} \cdot \left[\frac{\langle 0|\varphi|f_1\rangle\langle f_2|\varphi|0\rangle W_{f_2 f_1}^{0 0}}{\left(\omega - \left(\frac{E_{f_1} - E_0}{\hbar} \right) \right)^2 - \gamma_1\gamma_2 + W_{f_1 f_2}^{0 0} W_{f_2 f_1}^{0 0} - i(\gamma_1 + \gamma_2) \left(\omega - \frac{E_{f_1} - E_0}{\hbar} \right)} \right] \end{aligned}$$

Solution of equations (A.1) is

$$\begin{aligned} \mathcal{F}_1 &= \frac{i\mathcal{I}^2}{16e^2} \cdot \frac{\langle 0|\varphi|f_1\rangle\langle f_2|\varphi|0\rangle}{\left(\frac{E_{f_2} - E_{f_1}}{\hbar} \right)^2 - 4\gamma_1\gamma_2 - 2i(\gamma_1 + \gamma_2) \left(\frac{E_{f_2} - E_{f_1}}{\hbar} \right) + W_{f_1 f_2}^{f_1 f_2} W_{f_2 f_1}^{f_2 f_1}} \cdot \\ &\cdot \left[\frac{\left[\frac{E_{f_2} - E_{f_1}}{\hbar} - 2i\gamma_2 \right] W_{f_1 f_2}^{0 0}}{\left(\omega - \frac{E_{f_2} - E_0}{\hbar} \right)^2 - \gamma_1\gamma_2 + W_{f_1 f_2}^{0 0} W_{f_2 f_1}^{0 0} + i(\gamma_1 + \gamma_2) \left(\omega - \frac{E_{f_2} - E_0}{\hbar} \right)} \right. \\ &\left. - i \frac{W_{f_1 f_2}^{f_1 f_2} W_{f_2 f_1}^{0 0}}{\left(\omega - \frac{E_{f_1} - E_0}{\hbar} \right)^2 - \gamma_1\gamma_2 + W_{f_1 f_2}^{0 0} W_{f_2 f_1}^{0 0} - i(\gamma_1 + \gamma_2) \left(\omega - \frac{E_{f_1} - E_0}{\hbar} \right)} \right] \end{aligned} \quad (\text{A.3})$$

$$\begin{aligned} \mathcal{D}_1 &= \frac{i\mathcal{I}^2}{16e^2} \cdot \frac{\langle 0|\varphi|f_1\rangle\langle f_2|\varphi|0\rangle}{\left(\frac{E_{f_2} - E_{f_1}}{\hbar} \right)^2 - 4\gamma_1\gamma_2 - 2i(\gamma_1 + \gamma_2) \frac{E_{f_2} - E_{f_1}}{\hbar} + W_{f_1 f_2}^{f_1 f_2} W_{f_2 f_1}^{f_2 f_1}} \cdot \\ &\left[\frac{\left[\frac{E_{f_2} - E_{f_1}}{\hbar} - 2i\gamma_1 \right] W_{f_2 f_1}^{0 0}}{\left(\omega - \frac{E_{f_1} - E_0}{\hbar} \right)^2 - \gamma_1\gamma_2 + W_{f_1 f_2}^{0 0} W_{f_2 f_1}^{0 0} - i(\gamma_1 + \gamma_2) \left(\omega - \frac{E_{f_1} - E_0}{\hbar} \right)} \right. \\ &\left. - i \frac{W_{f_2 f_1}^{f_2 f_1} W_{f_1 f_2}^{0 0}}{\left(\omega - \frac{E_{f_2} - E_0}{\hbar} \right)^2 - \gamma_1\gamma_2 + W_{f_1 f_2}^{0 0} W_{f_2 f_1}^{0 0} + i(\gamma_1 + \gamma_2) \left(\omega - \frac{E_{f_2} - E_0}{\hbar} \right)} \right] \end{aligned} \quad (\text{A.4})$$

The explicit expression for the transition matrix elements $W_{f_1 f_2}^{f_1 f_2}$ and $W_{f_1 f_2}^{0 0}$ is given below

$$\begin{aligned} W_{f_1 f_2}^{f_1 f_2} &= \frac{\pi}{R_{eff}e^2} \left(1 + \tanh \left(\frac{E_{f_2} - E_{f_1}}{2k_B T} \right) \right) \frac{E_{f_2} - E_{f_1}}{\pi} \coth \left(\frac{E_{f_2} - E_{f_1}}{2k_B T} \right) |\langle f_1 | \exp^{i\frac{\varphi}{2}} | f_2 \rangle| \\ W_{f_1 f_2}^{0 0} &= \frac{\pi}{2R_{eff}e^2} \left(1 + \tanh \left(\frac{E_{f_2} - E_{f_1}}{4k_B T} \right) \right) \frac{E_{f_2} - E_{f_1}}{2\pi} \coth \left(\frac{E_{f_2} - E_{f_1}}{4k_B T} \right) \cdot \\ &\cdot \left[\langle 0 | \exp^{i\frac{\varphi}{2}} | 0 \rangle \langle f_1 | \exp^{-i\frac{\varphi}{2}} | f_2 \rangle + \langle 0 | \exp^{-i\frac{\varphi}{2}} | 0 \rangle \langle f_1 | \exp^{i\frac{\varphi}{2}} | f_2 \rangle \right] \end{aligned} \quad (\text{A.6})$$

$$W_{f_2 f_1}^{0 0} = \exp \left(-\frac{E_{f_2} - E_{f_1}}{2k_B T} \right) W_{f_1 f_2}^{0 0} \quad (\text{A.7})$$

Appendix B.

For the potential, given by eq.(2) we have

$$\begin{aligned}\varphi_{top} &= \varphi_x + \beta_L \sin(\varphi_{top}) \\ \frac{\partial \varphi_{top}}{\partial \varphi_x} &= -\frac{1}{\beta_L \cos(\varphi_{top}) - 1} \\ \frac{\partial U}{\partial \varphi_x} &= -U_0(\varphi - \varphi_x)\end{aligned}$$

$$\begin{aligned}U_1 &= \frac{U_0}{2} (\beta_L \cos(\varphi_{top}) - 1) \\ \frac{\partial U_1}{\partial \varphi_x} &= \frac{1}{2} \beta_L U_0 \frac{\sin(\varphi_{top})}{\beta_L \cos(\varphi_{top}) - 1}\end{aligned}$$

$$\begin{aligned}U_{top} &= U_0 \left[\frac{1}{2} (\varphi_{top} - \varphi_x)^2 + \beta_L \cos \varphi_{top} \right] \\ \frac{\partial U_{top}}{\partial \varphi_x} &= U_0 \left[\frac{\beta_L \sin \varphi_{top} - (\varphi_{top} - \varphi_x)}{\beta_L \cos(\varphi_{top}) - 1} - (\varphi_{top} - \varphi_x) \right]\end{aligned}$$

From equations (29), (32) we obtain all other derivatives that should be found for calculation of the quantities $\alpha_{1,2}$, $\beta_{1,2}$.

$$\frac{\partial \lambda}{\partial E} = -\sqrt{\frac{2M}{U_1}} \quad (B.1)$$

$$\frac{\partial \lambda}{\partial \varphi_x} = U_0 \sqrt{\frac{2M}{U_1}} \left[\frac{1}{\beta_L \cos(\varphi_{top}) - 1} \left[\beta_L \sin \varphi_{top} \left(1 - \frac{U_{top} - E}{4U_1} \right) - (\varphi_{top} - \varphi_x) \right] - (\varphi_{top} - \varphi_x) \right] \quad (B.2)$$

$$\frac{\partial \chi}{\partial \lambda} = \frac{1}{2} \psi \left(\frac{1}{2} \right) + \lambda^2 \sum_{k=0}^{\infty} \frac{1}{(2k+1)((2k+1)^2 + \lambda^2)} \quad (B.3)$$

Now by using equations (45), (46), (B.1), (B.1) we obtain the value of all coefficients α_1 , α_2 , β_1 , β_2 .

$$\beta_1 = \frac{\partial \Phi_1}{\partial E} + \frac{1}{2} \frac{\partial \chi}{\partial \lambda} \frac{\partial \lambda}{\partial E} = \sqrt{\frac{M}{2}} \int_{\tilde{\varphi}_1}^{\varphi_{top}} d\varphi \left(\frac{1}{\sqrt{U_{top} - U(\varphi)}} - \frac{\sqrt{\varphi_{top} - \tilde{\varphi}_1}}{(\varphi_{top} - \varphi) \sqrt{U_1(\varphi - \tilde{\varphi}_1)}} \right) \quad (B.4)$$

$$+ \sqrt{\frac{M}{2U_1}} \ln \left(\frac{8(MU_1)^{1/4}(\varphi_{top} - \tilde{\varphi}_1)}{2^{1/4}} \right) - \sqrt{\frac{M}{2U_1}} \frac{\partial \chi}{\partial \lambda}$$

$$\beta_2 = \frac{\partial \Phi_2}{\partial E} + \frac{1}{2} \frac{\partial \chi}{\partial \lambda} \frac{\partial \lambda}{\partial E} = \sqrt{\frac{M}{2}} \int_{\varphi_{top}}^{\tilde{\varphi}_4} d\varphi \left(\frac{1}{\sqrt{U_{top} - U(\varphi)}} - \frac{\sqrt{\tilde{\varphi}_4 - \varphi_{top}}}{(\varphi - \varphi_{top}) \sqrt{U_1(\tilde{\varphi}_4 - \varphi)}} \right) \quad (B.5)$$

$$+ \sqrt{\frac{M}{2U_1}} \ln \left(\frac{8(MU_1)^{1/4}(\tilde{\varphi}_4 - \varphi_{top})}{2^{1/4}} \right) - \sqrt{\frac{M}{2U_1}} \frac{\partial \chi}{\partial \lambda}$$

$$\alpha_1 = \frac{\partial \Phi_1}{\partial \varphi_x} + \frac{1}{2} \frac{\partial \chi}{\partial \lambda} \frac{\partial \lambda}{\partial \varphi_x} = U_0 \sqrt{\frac{M}{2}} \int_{\varphi_1}^{\varphi_2} d\varphi \frac{\varphi - \varphi_x}{\sqrt{E - U(\varphi)}} + \left(\frac{1}{2} \frac{\partial \chi}{\partial \lambda} + \frac{1}{4} \ln \left(\frac{2}{\lambda} \right) \right) U_0 \sqrt{\frac{2M}{U_1}} \quad (B.6)$$

$$\begin{aligned}
 & \cdot \left[\frac{1}{\beta_L \cos \varphi_{top} - 1} \left[\beta_L \sin \varphi_{top} \left(1 - \frac{U_{top} - E}{4U_1} \right) - (\varphi_{top} - \varphi_x) \right] - (\varphi_{top} - \varphi_x) \right] \\
 \alpha_2 &= \frac{\partial \Phi_2}{\partial \varphi_x} + \frac{1}{2} \frac{\partial \chi}{\partial \lambda} \frac{\partial \lambda}{\partial \varphi_x} = U_0 \sqrt{\frac{M}{2}} \int_{\varphi_3}^{\varphi_4} d\varphi \frac{\varphi - \varphi_x}{\sqrt{E - U(\varphi)}} + \left(\frac{1}{2} \frac{\partial \chi}{\partial \lambda} + \frac{1}{4} \ln \left(\frac{2}{\lambda} \right) \right) U_0 \sqrt{\frac{2M}{U_1}} \quad (\text{B.7}) \\
 & \cdot \left[\frac{1}{\beta_L \cos \varphi_{top} - 1} \left[\beta_L \sin \varphi_{top} \left(1 - \frac{U_{top} - E}{4U_1} \right) - (\varphi_{top} - \varphi_x) \right] - (\varphi_{top} - \varphi_x) \right]
 \end{aligned}$$

Appendix C.

Transition matrix elements between states close to the barrier top can be calculated in quasiclassical approximation if the parameter λ (see eq.(28)) is $\lambda \geq 1$. Consider first the matrix element $\langle L|\zeta|f_1\rangle$. With the help of eqs.(28), (40), (41) we obtain

$$\langle L|\zeta|f_1\rangle = \frac{1}{G_L G_{E_{f_1}}} \int_{\varphi_1(E_{f_1})}^{\varphi_2(E_{f_1})} d\varphi \frac{\sin\left(\pi/4 + \int_{\varphi_1(E_L)}^{\varphi} d\varphi \sqrt{2M(E_L - U(\varphi))}\right)}{(2M(E_L - U(\varphi)))^{1/4} (2M(E_{f_1} - U(\varphi)))^{1/4}} \zeta \sin\left(\pi/4 + \int_{\varphi_1(E_{f_1})}^{\varphi} d\varphi \sqrt{2M(E_{f_1} - U(\varphi))}\right)$$

that is equal to

$$\langle L|\zeta|f_1\rangle = \frac{1}{2G_L G_{E_{f_1}}} \int \frac{d\varphi}{\sqrt{2M(E_{f_1L} - U(\varphi))}} \zeta \cos\left((E_{f_1} - E_L) \int_{\varphi_1(E_{f_1L})}^{\varphi} \frac{Md\varphi}{\sqrt{2M(E_{f_1L} - U(\varphi))}}\right) \quad (C.2)$$

To calculate the last integral we can use the time variable t according to the classical equation of motion

$$\frac{M}{2} \left(\frac{\partial\varphi}{\partial t}\right)^2 = E - U(\varphi) \quad (C.3)$$

As a consequence, eq.(C.2) becomes

$$\langle L|\zeta|f_1\rangle = \frac{1}{2MG_L G_{E_{f_1}}} \int_0^{T_1/2} dt \zeta \cos\left(\frac{2\pi}{T_1} t \ell\right) \quad (C.4)$$

where T_1 is the period of the classical motion in the left potential well with energy E and ℓ is the number of states between energy levels E_{f_1} and E_L plus one. In our case $\ell = 1$. The initial value for φ is $\varphi(0) = \varphi_1$.

$$T_1 = 2M \int_{\varphi_3}^{\varphi_4} \frac{d\varphi}{\sqrt{2M(E - U(\varphi))}} \quad (C.5)$$

In the same way we obtain transition the matrix element $\langle R|\zeta|f_1\rangle$.

In eq.(C.1) $\varphi_1(E_{f_1})$ is the first crossing point of the energy level E_{f_1} in the left well and $\varphi_2(E_{f_1})$ is the second crossing point of the energy level E_{f_1} in the left well.

In the same way in eq.(C.2) $\varphi_1(E_{f_1L})$ is the first crossing point of the energy level E_{f_1L} in the left well, where E_{f_1L} is defined as

$$E_{f_1L} = \frac{E_{f_1} + E_L}{2} \quad (C.6)$$

Consider now the transition matrix element $\langle f_2|\zeta|f_1\rangle$. From eq.(28) we find

$$\langle f_2|\zeta|f_1\rangle = \frac{\hbar}{2G_{f_1} G_{f_2}} \left[\int_{\varphi_1}^{\varphi_2} d\varphi \frac{\zeta}{\sqrt{2M(E - U(\varphi))}} + B_{f_1} B_{f_2} \int_{\varphi_3}^{\varphi_4} d\varphi \frac{\zeta}{\sqrt{2M(E - U(\varphi))}} \right] \quad (C.7)$$

where $\varphi_{1,2,3,4}$ are the “turning points” and E here is $E = \frac{(E_{f_1} + E_{f_2})}{2}$. By using eq.(C.3) we reduce the expression (C.7) to the form

$$\langle f_2 | \zeta | f_1 \rangle = \frac{\hbar}{2MG_{f_1}G_{f_2}} \left[\int_0^{T_1/2} dt \zeta + B_{f_1} B_{f_2} \int_0^{T_2/2} dt \zeta \right] \quad (\text{C.8})$$

In eq.(C.8) the first integral is taken over the left potential well and the second one over the right potential well and T_1, T_2 are the periods of the classical motion in the left and in the right well respectively.

To improve eq.(C.8) we should take into account ortogonality of wavefunctions relative to the energies E_{f_1}, E_{f_2} . As result we obtain

$$\langle f_2 | \zeta | f_1 \rangle = \hbar \frac{1 - B_{f_1} B_{f_2}}{2MG_{f_1}G_{f_2}} \left[\frac{T_2}{T_1 + T_2} \int_0^{T_1/2} dt \zeta - \frac{T_1}{T_1 + T_2} \int_0^{T_2/2} dt \zeta \right] \quad (\text{C.9})$$

Acknowledgments

The research of one of us (Yu.N.O.) is supported by Cariplo Foundation-Italy, CRDF USA under Grant No. RP1-2565-MO-03 and the Russian Foundation of Basic Research. This work has been partially supported by MIUR under Project “Reti di Giunzioni Josephson per la Computazione e l’Informazione Quantistica-JOSNET”.

References

- [1] A. O. Caldeira and A. J. Leggett. *Phys. Rev. Lett.*, 46:211, 1981.
- [2] D. B. Schwartz, B. Sen, C. N. Archie, and J. E. Lukens. *Phys. Rev. Lett.*, 55:1547, 1985.
- [3] S. Washburn, R. A. Webb, R. F. Voss, and S. M. Faris. *Phys. Rev. Lett.*, 54:2712, 1985.
- [4] R. Rouse, S. Han, and J.E. Lukens. *Phys.Rev.Lett.*, 75:1614, 1995.
- [5] V. Corato, S.Rombetto, C. Granata, E. Esposito, L. Longobardi, M. Russo, R. Russo, B. Ruggiero, and P. Silvestrini. *Phys. Rev.*, B70:172502, 2004.
- [6] J. M. Martinis, M. H. Devoret, and J. Clarke. *Phys. Rev. Lett.*, 55:1543, 1985.
- [7] J. M. Martinis, M. H. Devoret, and J. Clarke. *Phys. Rev.*, 35:4682, 1987.
- [8] P. Silvestrini, V. G. Palmieri, B. Ruggiero, and M. Russo. *Phys. Rev. Lett.*, 79:3046, 1997.
- [9] J. R. Friedman, V. Patel, W. Chen, S. K. Tolpygo, and J. E. Lukens. *Nature (London)*, 406:43, 2000.
- [10] J. B. Majer, F. G. Paaauw, A.C. J. ter Haar, C. J. P.M. Harmans, and J. E. Mooij. *Phys. Rev. Lett.*, 94:090501, 2005.
- [11] J. Claudon, F. Balestro, F. W. J. Hekking, and O. Buisson. *Phys. Rev. Lett.*, 93:187003, 2004.
- [12] M. H. Devoret and J. M. Martinis. *Quantum Entanglement and Information Processing. - Les Houches Summer School Proceedings 79*. Elsevier, San Diego, CA., 2004.
- [13] N. Groenbech-Jensen and M. Cirillo. *Phys. Rev.*, B70:214507, 2004.
- [14] A.I.Larkin and Yu.N.Ovchinnikov. *J. of Low Temp. Phys.*, 63:317, 1986.
- [15] Yu.N.Ovchinnikov, P.Silvestrini, V.Corato, and S.Rombetto. *Phys. Rev.*, B71:024529, 2005.
- [16] Yu.N.Ovchinnikov and A.Schmid. *Phys. Rev.*, B50:6332, 1994.
- [17] D. Averin. *Solid State Commun.*, 105:659, 1998.
- [18] D. Averin. *Phys. of low temp. Phys.*, 118:781, 2000.
- [19] D. V. Averin, J. R. Friedman, and J. E. Lukens. *Phys. Rev.*, B62:11802, 2000.
- [20] A.I.Larkin and Yu.N.Ovchinnikov. *Sov. Phys. JETP*, 64:185, 1986.

- [21] A.I.Larkin and Yu.N.Ovchinnikov. *Phys. Rev.*, B50:6332, 1994.
- [22] U. Fano. *Rev. of Mod. Phys.*, 29:74, 1957.
- [23] A. Barone and G. Paternó. *Physics and Applications of the Josephson Effect*. Wiley, New York, 1982.
- [24] A.I.Larkin and Yu.N.Ovchinnikov. *Sov. Phys. JETP*, 60:1060, 1984.
- [25] I. M. Ryzhik and I. S. Gradshteyn. *Table of Integrals, Series and Products*. Academic Press, New York, 1965.
- [26] L. Landau and L. Lifshitz. *Quantum Mechanics: non-relativistic theory*. Butterworth-Heinemann, 1981.
- [27] P. Silvestrini, B. Ruggiero, and Yu.N. Ovchinnikov. *Phys. Rev.*, B54:1246, 1996.